The Plant Cell, Vol. 28: 568–582, February 2016, www.plantcell.org

Reconstitution of CO_2 Regulation of SLAC1 Anion Channel and Function of CO_2-Permeable PIP2;1 Aquaporin as CARBONIC ANHYDRASE4 Interactor

Cun Wang,[a,1] Honghong Hu,[a,b,1,2] Xue Qin,[c] Brian Zeise,[c] Danyun Xu,[b] Wouter-Jan Rappel,[d] Walter F. Boron,[c] and Julian I. Schroeder[a,2]

[a] Division of Biological Sciences, Section of Cell and Developmental Biology, University of California San Diego, La Jolla, California 92093-0116

[b] College of Life Science and Technology, Huazhong Agricultural University, Wuhan 430070, China

[c] Department of Physiology and Biophysics, Case Western Reserve University, Ohio 44106

[d] Physics Department, University of California San Diego, La Jolla, California 92093

ORCID IDs: 0000-0001-6975-0959 (C.W.); 0000-0003-0538-6646 (H.H.); 0000-0001-8049-6285 (X.Q.)

Dark respiration causes an increase in leaf CO_2 concentration (*Ci*), and the continuing increases in atmospheric [CO_2] further increases *Ci*. Elevated leaf CO_2 concentration causes stomatal pores to close. Here, we demonstrate that high intracellular CO_2/HCO_3^- enhances currents mediated by the *Arabidopsis thaliana* guard cell S-type anion channel SLAC1 upon coexpression of any one of the Arabidopsis protein kinases OST1, CPK6, or CPK23 in *Xenopus laevis* oocytes. Split-ubiquitin screening identified the PIP2;1 aquaporin as an interactor of the βCA4 carbonic anhydrase, which was confirmed in split luciferase, bimolecular fluorescence complementation, and coimmunoprecipitation experiments. PIP2;1 exhibited CO_2 permeability. Mutation of *PIP2;1* in planta alone was insufficient to impair CO_2- and abscisic acid-induced stomatal closing, likely due to redundancy. Interestingly, coexpression of βCA4 and PIP2;1 with OST1-SLAC1 or CPK6/23-SLAC1 in oocytes enabled extracellular CO_2 enhancement of SLAC1 anion channel activity. An inactive PIP2;1 point mutation was identified that abrogated water and CO_2 permeability and extracellular CO_2 regulation of SLAC1 activity. These findings identify the CO_2-permeable PIP2;1 as key interactor of βCA4 and demonstrate functional reconstitution of extracellular CO_2 signaling to ion channel regulation upon coexpression of PIP2;1, βCA4, SLAC1, and protein kinases. These data further implicate SLAC1 as a bicarbonate-responsive protein contributing to CO_2 regulation of S-type anion channels.

INTRODUCTION

Plant stomata, which are formed by pairs of guard cells in the epidermis of aerial tissues, control gas exchange and transpiration. Stomatal movements are regulated by several signals, including the phytohormone abscisic acid (ABA), CO_2, humidity, reactive oxygen species, light, and pathogens (Hetherington and Woodward, 2003; Kim et al., 2010; Roelfsema et al., 2012; Murata et al., 2015). Daily respiration during darkness causes a rapid elevation in the CO_2 concentration in the intercellular space in leaves (*Ci*) to ≥600 ppm (Hanstein et al., 2001). Furthermore, the continuing increase in the atmospheric CO_2 concentration also causes an increase in *Ci*. Increased *Ci* reduces stomatal apertures and thus affects CO_2 influx into plants, leaf heat stress, plant water use efficiency, and yield (LaDeau and Clark, 2001; Medlyn et al., 2001; Hetherington and Woodward, 2003; Ainsworth and Long, 2005; Battisti and Naylor, 2009; Holden, 2009; Frommer, 2010).

Carbonic anhydrases accelerate the reaction: $CO_2 + H_2O <-> HCO_3^- + H^+$. Double mutant plants in the *Arabidopsis thaliana* β-carbonic anhydrases (*βca1* and *βca4*) exhibit slowed stomatal movement responses to CO_2 changes (Hu et al., 2010). Expression of an unrelated mammalian α-CA in the *βca1 βca4* double mutant guard cells restores the stomatal CO_2 response, suggesting that CA-mediated CO_2 catalysis to bicarbonate and protons in guard cells is an important step for transmission of the CO_2 signal (Hu et al., 2010).

SLAC1 (*SLOW ANION CHANNEL-ASSOCIATED1*) encodes an S-type anion channel in Arabidopsis guard cells (Negi et al., 2008; Vahisalu et al., 2008). A group of protein kinases including OST1 (OPEN STOMATA1), CPKs (Ca^{2+}-dependent protein kinases), and GUARD CELL HYDROGEN PEROXIDE-RESISTANT1 can phosphorylate and activate SLAC1 anion channels in *Xenopus laevis* oocytes (Geiger et al., 2009, 2010; Lee et al., 2009; Brandt et al., 2012; Hua et al., 2012). S-type anion channels are permeable to Cl^- and NO_3^-, but not to HCO_3^- (Schmidt and Schroeder, 1994; Geiger et al., 2009; Xue et al., 2011). Intracellular bicarbonate generated by carbonic anhydrases acts as a second messenger and activates S-type anion channels in guard cells (Xue et al., 2011; Tian et al., 2015).

The OST1 protein kinase is required for CO_2-induced stomatal closing (Xue et al., 2011; Merilo et al., 2013). A recent study reported that RHC1, a MATE-type transporter protein, acts as a bicarbonate sensor (Tian et al., 2015) and also inhibits HIGH

[1] These authors contributed equally to this work.

[2] Address correspondence to huhh@mail.hzau.edu.cn or jischroeder@ucsd.edu.

The author responsible for distribution of materials integral to the findings presented in this article in accordance with the policy described in the Instructions for Authors (www.plantcell.org) is: Julian I. Schroeder (jischroeder@ucsd.edu).

www.plantcell.org/cgi/doi/10.1105/tpc.15.00637

LEAF TEMPERATURE1 (HT1), a protein kinase that negatively regulates CO_2-induced stomatal closing (Hashimoto et al., 2006). HT1 was found to phosphorylate and inhibit the OST1 protein kinase (Tian et al., 2015). Here, we pursued investigation of the molecular targets and requirements for intracellular CO_2/HCO_3^- enhancement of SLAC1 anion channel activity.

We show that elevated intracellular $NaHCO_3$ can enhance SLAC1 anion channel currents in both OST1-SLAC1- and CPK6/23-SLAC1-expressing oocytes. We isolate and characterize the PIP2;1 aquaporin as a new βCA4 carbonic anhydrase interactor and as a CO_2-permeable aquaporin. In addition, we show that extracellular CO_2 enhancement of S-type anion channels can be reconstituted when OST1-SLAC1 or CPK6/23-SLAC1 are coexpressed with the βCA4 carbonic anhydrase and PIP2;1 in *X. laevis* oocytes.

RESULTS

Elevated Intracellular $NaHCO_3$ Can Enhance SLAC1 Anion Channel Currents in Oocytes Expressing OST1-SLAC1

Intracellular bicarbonate enhances S-type anion channel currents in wild-type Arabidopsis guard cells (Hu et al., 2010; Xue et al., 2011; Tian et al., 2015). To test for minimal requirements by which bicarbonate could regulate the S-type anion channel SLAC1, we expressed SLAC1yc, or coexpressed SLAC1yc with the OST1yn protein kinase in *X. laevis* oocytes. To investigate electrophysiological responses, we injected 11.5 mM $NaHCO_3$ into oocytes, mimicking high bicarbonate conditions that activate S-type anion channel currents in guard cells (Hu et al., 2010; Xue et al., 2011). Injection of 11.5 mM $NaHCO_3$ buffered to pH 7.5 with Mes/Tris corresponds to 10.5 mM free HCO_3^- and 1 mM free CO_2 (see Methods). Results from over six independent oocyte batches showed that high $NaHCO_3$ consistently enhanced SLAC1yc/OST1yn-mediated anion channel currents in oocytes (Figure 1; $P = 0.027$ at -160 mV in SLAC1yc/OST1yn versus SLAC1yc/OST1yn + HCO_3^-). By contrast, SLAC1yc expression alone or water-injected control oocytes showed no significant $NaHCO_3$ activation (Figure 1). Controls were included in oocyte batches to ensure that oocyte injection of $NaHCO_3$ or water without protein kinases did not give rise to significant current increases in the analyzed oocyte batches (e.g., Figure 1; >300 control oocytes in total). In additional control experiments with a different recording buffer containing 96 mM NaCl in the bath, the reversal potential of SLAC1yc/OST1yn + HCO_3^--mediated currents shifted consistent with the chloride equilibrium potential (Supplemental Figure 1B).

To determine whether this activation is pH dependent, we also injected 11.5 mM $NaHCO_3$ buffered to pH 7.0 and pH 8.0 into oocytes. The results showed that pH had no effect on the activation of SLAC1-mediated anion channel currents (Supplemental Figure 1). In additional experiments, we injected an iso-osmotic 23 mM sorbitol solution buffered to pH 8. No enhancement of SLAC1-mediated ionic currents was observed, suggesting that a pH change was not the mechanism mediating the enhancement of SLAC1-mediated currents. As an additional control for $NaHCO_3$, injection of NaCl at the same concentration into oocytes did not enhance SLAC1yc/OST1yn-mediated anion channel currents, but rather showed an average reduction in anion currents (Supplemental Figure 2).

We investigated whether the $NaHCO_3$-induced enhancement of SLAC1yc/OST1yn-mediated anion channel currents was dependent on the $NaHCO_3$ concentration. A series of final intracellular $NaHCO_3$ concentrations was microinjected: 0, 1, 5.7, and 11.5 mM. Results from over three independent oocyte batch experiments showed that low $NaHCO_3$ failed to significantly enhance SLAC1yc/OST1yn-mediated anion channel currents under the imposed conditions, while injection of high $NaHCO_3$ concentrations (5.7 and 11.5 mM) enhanced SLAC1yc/OST1yn-mediated anion channel currents (Figures 2A and 2B), which is in line with required $NaHCO_3$ concentrations in guard cells (Xue et al., 2011; Tian et al., 2015). Furthermore, activation by 11.5 mM $NaHCO_3$ was stronger than by 5.7 mM $NaHCO_3$ (Figures 2A and 2B; $P = 0.034$ at -160 mV in 11.5 mM $NaHCO_3$ versus 5.7 mM $NaHCO_3$). Thus, high intracellular $NaHCO_3$ concentrations could enhance SLAC1yc/OST1yn-mediated anion channel currents at similar concentrations as in guard cells (Xue et al., 2011).

PIP2;1 Aquaporin Interacts with βCA4 Carbonic Anhydrase and Is a CO_2-Permeable Aquaporin

The βCA1 and βCA4 carbonic anhydrases function in CO_2-induced stomatal closing (Hu et al., 2010, 2015). To characterize the CO_2 signaling mechanisms mediated by carbonic anhydrase proteins, we screened for interactors of these β-carbonic anhydrases using the yeast two-hybrid system with an Arabidopsis cDNA library (BD Clontech) and full-length βCA4 cDNA as bait. However, no reproducible candidate interactors were isolated. The βCA4 carbonic anhydrase is localized at the plasma membrane in transiently transformed *Nicotiana benthamiana* cells (Fabre et al., 2007; Hu et al., 2010) and in guard cells (Hu et al., 2015). By contrast, βCA1 is targeted to chloroplasts (Fabre et al., 2007; Hu et al., 2015). To screen for putative plasma membrane interactors of the carbonic anhydrase βCA4, the split-ubiquitin system (SUS) was developed and improved to detect protein-protein interactions (Jones et al., 2014a). We used βCA4 as a bait and screened a SUS cDNA library, which was constructed in the pNX33-DEST vector (Grefen et al., 2007). In this screen, reproducible putative βCA4-interacting proteins were isolated, including Nodulin MtN3 (At3g06433), CNGC13 (At3g01010), and the PIP2;1 aquaporin (Figure 3A).

To further investigate putative interactors of βCA4 and assess whether these interactions occur in vivo, PIP2;1 aquaporin was chosen for further analyses in this study. The split YFP combinations of βCA4-YC with PIP2;1-YN were transiently coexpressed in *N. benthamiana* leaves. Bimolecular fluorescence complementation (BiFC) (Walter et al., 2004; Bracha-Drori et al., 2004) results indicated that βCA4-YC and PIP2;1-YN interacted with each other in the vicinity of the plasma membrane (Figure 3B), supporting the SUS results. Reversible split luciferase complementation assays (Chen et al., 2008) were conducted to further test protein-protein interactions in *N. benthamiana* leaves and also showed that βCA4 interacts with PIP2;1 (Figure 3C). Furthermore, coimmunoprecipitation experiments were performed to test for protein-protein interactions in *N. benthamiana* leaves. βCA4-YFP coimmunoprecipitated with PIP2;1-HA as detected using HA and GFP antibodies (Figure 3D). In summary, four independent approaches, SUS, BiFC, split luciferase complementation, and coimmunoprecipitation, showed interactions of βCA4 and PIP2;1 in vitro and in plant cells.

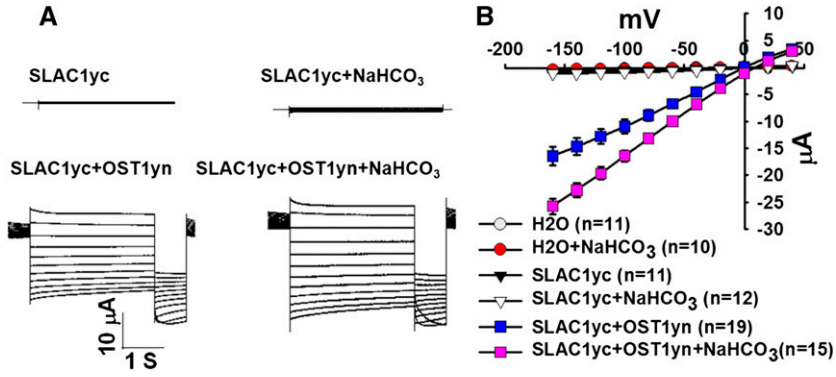

Figure 1. Injection of 11.5 mM $NaHCO_3$ into Oocytes Causes Enhancement of SLAC1-Mediated Anion Channel Currents When SLAC1 Is Coexpressed with OST1, While SLAC1 Expression Alone or Water-Injected Oocytes Did Not Show Significant HCO_3^- Regulation.

(A) Whole-cell currents were recorded from oocytes expressing the indicated cRNAs. During recordings of SLAC1 anion currents, single voltage pulses were applied in −20-mV decrements from +40 to −160 mV for 4 s, and the holding potential was 0 mV.

(B) Steady state current-voltage relationships from oocytes recorded as in **(A)**. Numbers of oocytes recorded for each condition in the same batch of oocytes are provided in the current-voltage panels in all figures. Data are mean ± SE. For some data points, the symbols are larger than the SE in **(B)**. Results from over six independent batches of oocytes showed similar results.

The aquaporins Nt-AQP1 from tobacco, PIP1;2 from Arabidopsis, and four PIP2 proteins in barley (*Hordeum vulgare*) have been identified as CO_2 transporters in plant cells (Uehlein et al., 2003, 2008, 2012; Mori et al., 2014). We investigated whether PIP2;1 can also mediate CO_2 transport. PIP2;1 was expressed in *X. laevis* oocytes. Extracellular pH changes in the proximity of the plasma membrane (ΔpH) were used as an indicator of the changes in acidification at the membrane surface of *X. laevis* oocytes mediated by CO_2 flux (Musa-Aziz et al., 2009, 2014). Expression of PIP2;1 resulted in an enhanced change in the surface pH of oocytes, indicating that PIP2;1 enhanced the CO_2 permeability of oocytes over the background CO_2 permeability (Figure 3E; Supplemental Figure 3). Interestingly, when PIP2;1 was coexpressed with βCA4 in *X. laevis* oocytes, ΔpH was significantly increased compared with PIP2;1 suggesting enhanced CO_2 transport into oocytes (Figure 3E; Supplemental Figure 3). Furthermore, βCA4 expression alone also significantly enhanced ΔpH changes compared with water-injected control oocytes (Figure 3E; Supplemental Figure 3), which is similar to human α-carbonic anhydrase II-enhanced CO_2 flux across the *X. laevis* oocyte plasma membrane (Musa-Aziz et al., 2014).

Reconstitution of Extracellular CO_2 Signaling to SLAC1 Anion Channel Regulation

As βCA4 physically interacts with the PIP2;1 aquaporin (Figures 3A to 3D) and PIP2;1 shows a CO_2 permeability (Figure 3E), we pursued experiments to investigate whether extracellular CO_2/HCO_3^- regulation of anion channels can be reconstituted in *X. laevis* oocytes.

Although injection of $NaHCO_3$ into oocytes enhanced SLAC1-mediated currents (Figures 1 and 2), increasing extracellular CO_2/HCO_3^- by addition of 11.5 mM $NaHCO_3$ to the bath solution did not enhance SLAC1yc/OST1yn-expressing oocyte currents (Figure 4A). When either βCA4 or the PIP2;1 aquaporin alone were coexpressed with SLAC1yc and OST1yn in *X. laevis* oocytes in the presence of high CO_2/HCO_3^- in the bath solution, no significant increase in ion currents was observed in three independent batches of oocytes (Figure 4B). We then coexpressed βCA4 and PIP2;1 with SLAC1yc and OST1yn in oocytes and found that βCA4 and PIP2;1 did not significantly enhance ion currents without extracellular addition of $NaHCO_3$ (Figure 4C). By contrast, in more than four independent batches of oocytes in the presence of extracellular $NaHCO_3$, coexpression of βCA4, PIP2;1, SLAC1yc, and OST1yn in oocytes resulted in larger anion channel currents than those in SLAC1yc/OST1yn coexpressing oocytes (Figures 4D and 4E; P = 0.017 at −160 mV in SLAC1yc/OST1yn versus SLAC1yc/OST1yn+CA4+PIP2;1).

Functional PIP2;1 Is Required for the Extracellular CO_2 Response

To test the hypothesis that a functional PIP2;1 is required for the extracellular CO_2 response, we attempted to design non-permeable PIP2;1 isoforms. Several aquaporin structures have been resolved by x-ray crystallography, including human AQP1, human AQP5, and spinach (*Spinacia oleracea*) aquaporin PIP2 (Ren et al., 2000; Fujiyoshi et al., 2002; Kukulski et al., 2005; Horsefield et al., 2008; Nyblom et al., 2009). We aligned hAQP1, hAQP5, and So-PIP2 with At-PIP2;1, and based on this model, we speculated that L81, W85, and F210 might play a role in CO_2 permeability. These three PIP2;1 amino acid residues were mutated to alanine in PIP2;1, and the cRNAs were expressed in *X. laevis* oocytes. In addition, oocytes expressing grapevine (*Vitis vinifera*) PIP2;5 have a very low water permeability compared with those expressing Vv-PIP2;1 or So-PIP2;1 (Shelden et al., 2009). Previous sequence alignments of the conserved B loop led to the model that W100 is a large and hydrophobic residue that may block the pore of Vv-PIP2;5 (Shelden et al., 2009). We therefore mutated the corresponding residue in PIP2;1-G103 to W. The osmotic water permeability (Pf) of PIP2;1-L81A, PIP2;1-W85A, and PIP2;1-F210A showed no significant difference compared

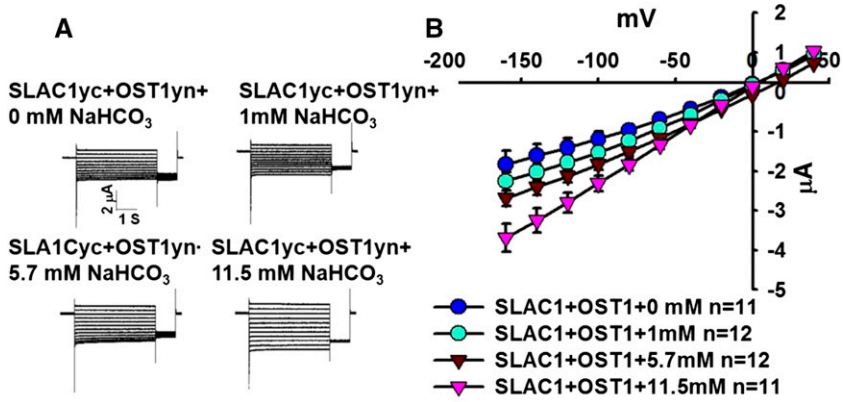

Figure 2. $NaHCO_3$ Concentration-Dependent Enhancement of SLAC1-Mediated Anion Channel Currents When SLAC1 Was Coexpressed with OST1 in *X. laevis* Oocytes.

(A) Whole-cell currents were recorded from oocytes after injection of the indicated final concentrations of $NaHCO_3$.
(B) Steady state current-voltage relationships from oocytes recorded as in **(A)**. Data are mean ± SE. For some data points, the symbols are larger than the SE. Results from three independent oocyte batches showed similar results.

with the water permeability of wild-type PIP2;1 (Figure 5A). Interestingly, the PIP2;1-G103W point mutant isoform exhibited a much weaker water permeability than wild-type PIP2;1 in *X. laevis* oocytes (Figure 5A). This supports the model that the PIP2;1-G103 residue is important for PIP2;1-mediated function.

To determine whether the PIP2;1 mutant protein isoforms are expressed and translocated to the plasma membrane of *X. laevis* oocytes, mRNAs of PIP2;1-YFP fusion proteins were expressed in oocytes. Confocal fluorescence microscopy analyses showed that all tested PIP2;1 mutant isoforms, including the nonfunctional PIP2;1-G103W-YFP fusion protein, were present at the plasma membrane (Figure 5B).

We next coexpressed the four mutant PIP2;1 isoforms with βCA4, SLAC1yc and OST1yn in *X. laevis* oocytes. We found that expression of the mutants PIP2;1-L81A, PIP2;1-W85A, and PIP2;1-F210A could still mediate extracellular CO_2/HCO_3^- enhancement of SLAC1yc/OST1yn-mediated anion channel currents in four independent oocyte batches (Figure 6; Supplemental Figure 4). By contrast, the PIP2;1-G103W mutant isoforms did not enable extracellular CO_2/HCO_3^--mediated enhancement SLAC1yc/OST1yn-mediated anion channel currents in three independent oocyte batches (Figure 6; Supplemental Figure 4).

The PIP2;1-G103W mutation disrupted water permeability but not plasma membrane localization of PIP2;1 in *X. laevis* oocytes (Figure 5B). We investigated whether PIP2;1-G103W affects CO_2 transport in oocytes. Experiments showed that expression of PIP2;1 resulted in an enhanced change in surface pH of oocytes, whereas in the same oocyte batches, PIP2;1-G103W did not significantly change the surface pH compared with control oocytes (Figure 5C). These results suggested that the G103W mutation impaired PIP2;1-mediated transport of both water and CO_2 (see Discussion).

Surface pH changes of oocytes suggested that PIP2;1 and βCA4 coexpression together enhanced CO_2 transport into oocytes more than expression of either protein alone (Figure 3E). We pursued mathematical modeling (Somersalo et al., 2012) to simulate PIP2;1 as enhancing the oocyte plasma membrane CO_2 permeability and βCA4 as enhancing CO_2 catalysis in oocytes. We modeled the response of an oocyte following a sudden increase in external CO_2 concentration (see Methods). Simulations were started with the internal CO_2 concentration set to 200 ppm and the external concentration increased from 200 to 800 ppm (Hu et al., 2015). This sudden jump results in an influx of CO_2 and a transient increase in the membrane surface pH, pH_s (Supplemental Figure 5).

Simulations show the predicted pH_s as a function of time for an oocyte under our baseline parameters (i.e., low membrane permeability and no carbonic anhydrase-mediated acceleration of CO_2 catalysis) as a black line (Supplemental Figure 5). Consistent with the results of Somersalo et al. (2012), the predicted pH_s increased and reached a transient maximum. The effect of carbonic anhydrases was simulated by setting an acceleration factor for CO_2 catalysis in the interior of oocytes. As a result of the accelerated dynamics, the predicted CO_2 influx was increased, resulting in an increase in the pH_s values (Supplemental Figure 5). We also simulated the effect of PIP2;1 expression, without the presence of CA, by increasing the membrane permeability to $P_{M,CO2}$ = 10 cm/s. As expected, this increase in membrane permeability increased the predicted CO_2 influx and the peak value of pH_s (green line). Finally, we modeled the combined effects of PIP2;1 and carbonic anhydrase coexpression by setting $P_{M,CO2}$ = 10 cm/s and F = 100. Consistent with the experimental data, this combination led to an even higher predicted increase in ΔpH_s (blue line). Thus, this model for CO_2 dynamics can capture the relative larger increase in ΔpH_s upon coexpression of PIP2;1 and CA. Based on this and the experimental results (Figures 3E and 6; Supplemental Figures 3 and 4), a threshold CO_2 influx may be required to produce a measurable change in SLAC1 activity.

PIP2;1 Mutation Alone Does Not Significantly Impair CO_2 and ABA Regulation of Stomatal Movements

To explore whether insertional mutation in the *PIP2;1* gene in Arabidopsis alone is sufficient to impair CO_2 regulation of stomatal movements, we pursued stomatal conductance analyses in response to CO_2 concentration changes in *PIP2;1* T-DNA mutant

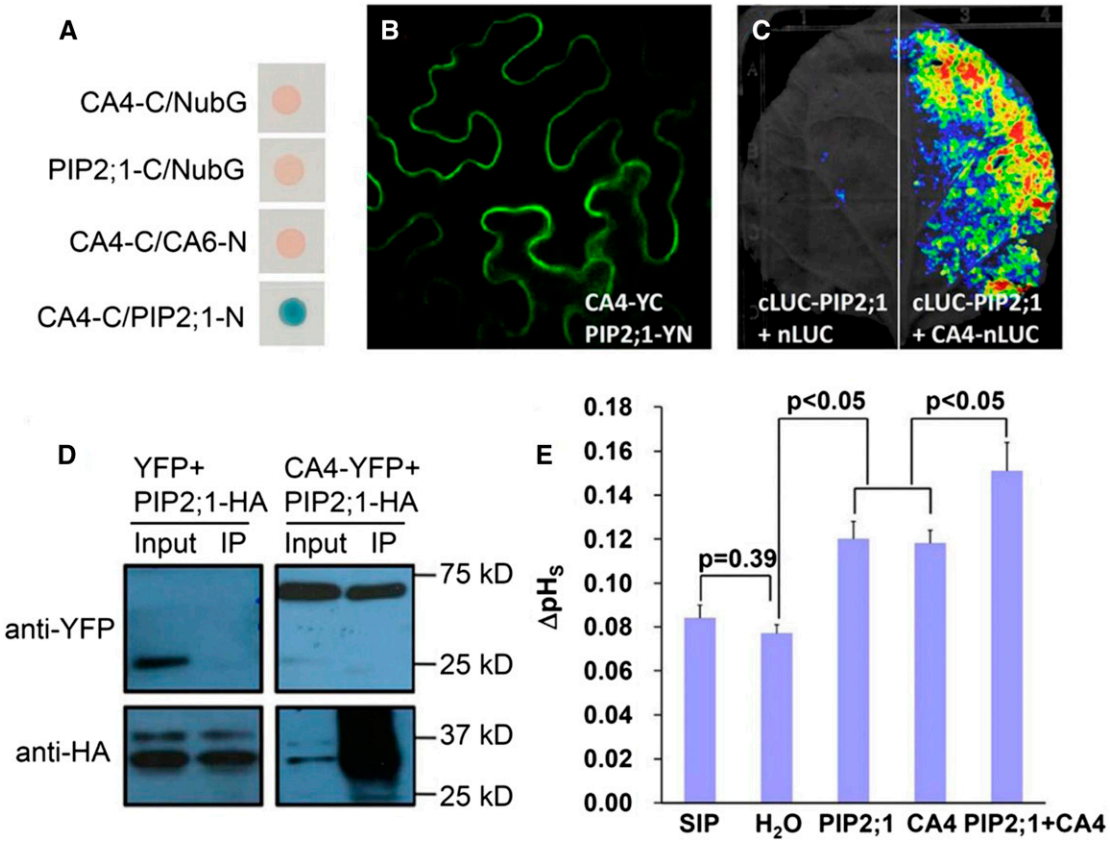

Figure 3. The Carbonic Anhydrase βCA4 Interacts with the PIP2;1 Protein and βCA4 Increases the CO_2 Permeability Mediated by PIP2;1.

(A) The aquaporin PIP2;1 was identified as a βCA4-interacting protein by screening a split ubiquitin yeast two-hybrid library. Interactions are shown in blue on the medium plus X-Gal substrate. βCA6 and soluble NubG were used as negative controls.

(B) and **(C)** Split YFP **(B)** and reversible split luciferase complementation assays **(C)** showed that βCA4 interacts with PIP2;1 at the plasma membrane in tobacco leaves. Note that reversible split luciferase assays do not permit single-cell resolution and a whole leaf is shown in **(C)**. In **(C)**, left, cLUC-PIP2;1 with only nLUC was used as negative control and showed no clear luciferase bioluminescence signal.

(D) Coimmunoprecipitation experiments show an interaction of βCA4 with the PIP2;1 aquaporin. Crude protein extracts from inoculated *N. benthamiana* leaves were used for immunoprecipitation as an input. Input protein was immunoprecipitated with anti-HA matrix. The input and immunoprecipitate (IP) were probed with anti-HA or anti-GFP antibodies as indicated.

(E) βCA4 and PIP2;1 enhance the CO_2 permeability of *X. laevis* oocytes as analyzed by membrane surface changes in pH (pH_s). SIP1A- (At3g04090) and water-injected oocytes serve as control injections (*$P < 0.05$). Error bar is one SE of the mean. Tukey method for pair comparison in the ANOVA was used for statistical tests.

plants. However, *pip2;1* mutant leaves showed similar stomatal responses to CO_2 changes as wild-type leaves (Figures 7A and 7B).

A recent study reported that *PIP2;1* T-DNA insertion mutant plants are impaired specifically in ABA-induced stomatal closure (Grondin et al., 2015). We also investigated whether PIP2;1 is involved in the ABA-induced stomatal closing pathway, since the same aquaporins are known to transport water and CO_2 (Figures 3E and 5) (Mori et al., 2014). Genotype-blind stomatal movement imaging analyses of individually mapped stomata showed that *pip2;1* single mutant stomata retained intact responses to 10 μM ABA treatment in time-course analyses of ABA-induced stomatal closing (Figure 7C). Furthermore, we also tested the effect of ABA on a previously described *pip2;1* mutant, *pip2;1-2* (Da Ines et al., 2010; Grondin et al., 2015) in parallel, but stomata in both *pip2;1* and *pip2;1-2* mutant leaf epidermal layers closed to similar levels as the wild type 1 h after ABA treatment (Figure 7D). These data indicated that PIP2;1 mutation alone was insufficient under the imposed conditions to impair the ABA-induced stomatal closing pathway. These findings may be related to coexpression of multiple *PIP* homologs in Arabidopsis guard cells (Yang et al., 2008; Zhao et al., 2008; Bauer et al., 2013) and overlapping gene functions.

SLAC1 Is Likely to Serve as a Bicarbonate-Responsive Protein

Our findings show that high intracellular bicarbonate could enhance SLAC1yc/OST1yn-mediated anion channel currents in *X. laevis* oocytes. These data indicated that either the OST1 protein kinase or SLAC1 or both proteins together may function as a bicarbonate-responsive protein. To determine whether OST1 is

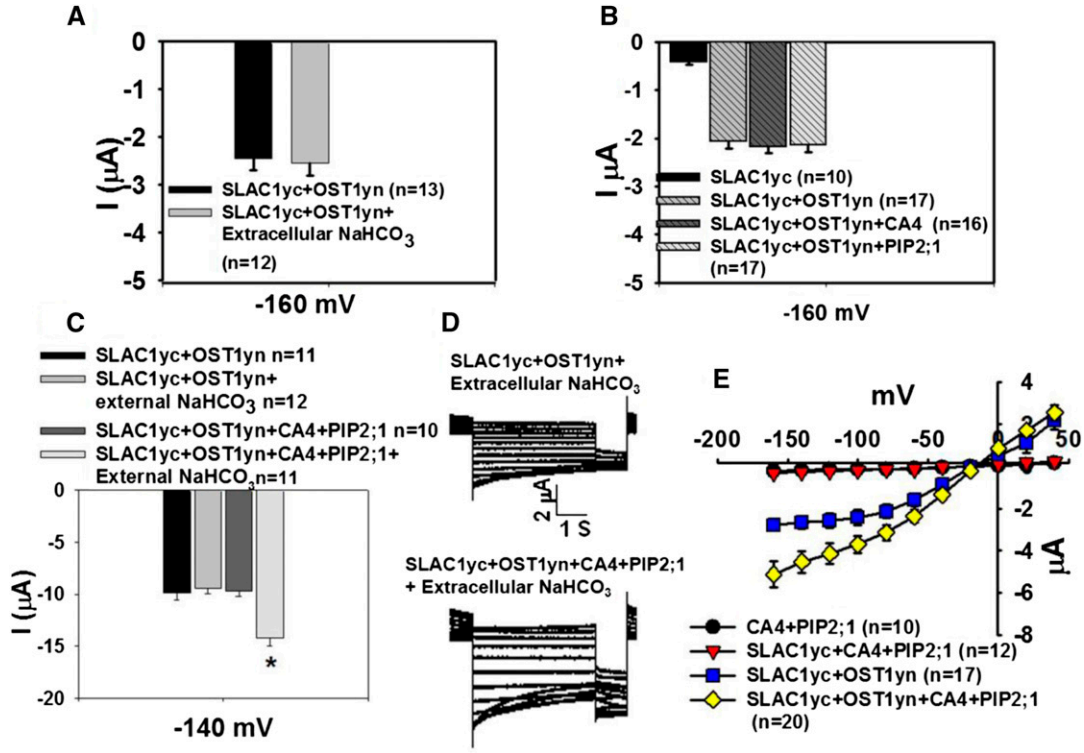

Figure 4. Reconstitution of Extracellular CO_2/HCO_3^- Enhancement of SLAC1-Mediated Anion Currents Requires PIP2;1 and βCA4 in *X. laevis* Oocytes.

(A) Increasing extracellular CO_2/HCO_3^- by addition of 11.5 mM $NaHCO_3$ did not enhance currents in SLAC1yc/OST1yn-expressing oocytes.
(B) Either βCA4 or PIP2;1 expressed alone together with SLAC1 and OST1 did not suffice to enhance SLAC1-mediated anion channel currents in *X. laevis* oocytes. Data in **(A)** and **(B)** are shown at −160 mV as mean ± SE.
(C) Coexpression of βCA4 and PIP2;1 with SLAC1yc/OST1yn did not significantly enhance ion currents in the bath solution without high CO_2/HCO_3^- but showed enhanced currents upon extracellular $NaHCO_3$ application.
(D) Whole-cell currents were recorded from oocytes coexpressing the indicated cRNAs. βCA4 and PIP2;1 coexpression enhanced SLAC1/OST1-mediated anion channel currents in the presence of 11.5 mM $NaHCO_3$ in the bath solution.
(E) Steady state current-voltage relationships from oocytes recorded as in **(D)**. Data are mean ± SE. The results were found in at least three independent batches of oocytes.

essential for the CO_2/HCO_3^- response, we coexpressed SLAC1 with the protein kinases CPK6 or CPK23 in *X. laevis* oocytes, as these protein kinases are established to activate SLAC1 in *X. laevis* oocytes (Geiger et al., 2010; Brandt et al., 2012). Four independent batches of oocytes showed that injection of high intracellular $NaHCO_3$ or extracellular CO_2/HCO_3^- and coexpression of βCA4 and PIP2;1 with SLAC1 and CPK6 or CPK23 could enhance SLAC1 anion channel currents (Figure 8). Together, these findings indicate that SLAC1 is likely to play the role of a bicarbonate-responsive protein, but SLAC1 requires a protein kinase to mediate channel activity.

RHC1 Expression Alone in Oocytes Produces Ionic Currents That Are Not Affected by $NaHCO_3$ or OST1

During the course of this research, another study identified the MATE transporter RHC1 as a candidate HCO_3^- sensor when coexpressed with SLAC1, OST1, and HT1 in *X. laevis* oocytes (Tian et al., 2015). However, HCO_3^- effects on oocytes expressing RHC1 alone or on oocytes expressing only OST1 and SLAC1 were not investigated. A full-length *RHC1* cDNA was obtained from a plant membrane protein cDNA collection (Jones et al., 2014a). We then expressed the *RHC1* cRNA in *X. laevis* oocytes with or without OST1. Unexpectedly, when expressing RHC1 alone, oocytes showed ionic currents (Figure 9). The RHC1 MATE transporter-mediated currents were not affected by injection of 11.5 mM $NaHCO_3$ into *X. laevis* oocytes in the presence or absence of OST1, and OST1 did not enhance RHC1-mediated currents (Figure 9).

DISCUSSION

The carbonic anhydrase βCA4 is involved in CO_2-induced stomatal closing (Hu et al., 2010, 2015). In further investigating the CO_2 signaling mechanisms mediated by the βCA4 protein, we found that βCA4 interacted with PIP2;1. The interaction of PIP2;1 with βCA4 may explain why βCA4 has been found to be located at the intracellular side of the plasma membrane in plant cells, including in guard cells even though βCA4 does not have a transmembrane domain (Fabre et al., 2007; Hu et al., 2015). It has been widely demonstrated that CO_2 is transported across membranes via aquaporins: The AQP1 aquaporin from tobacco displays CO_2 transport activity in *X. laevis* oocytes (Uehlein et al., 2003). The Arabidopsis PIP1;2 aquaporin displays CO_2 permeability in yeast

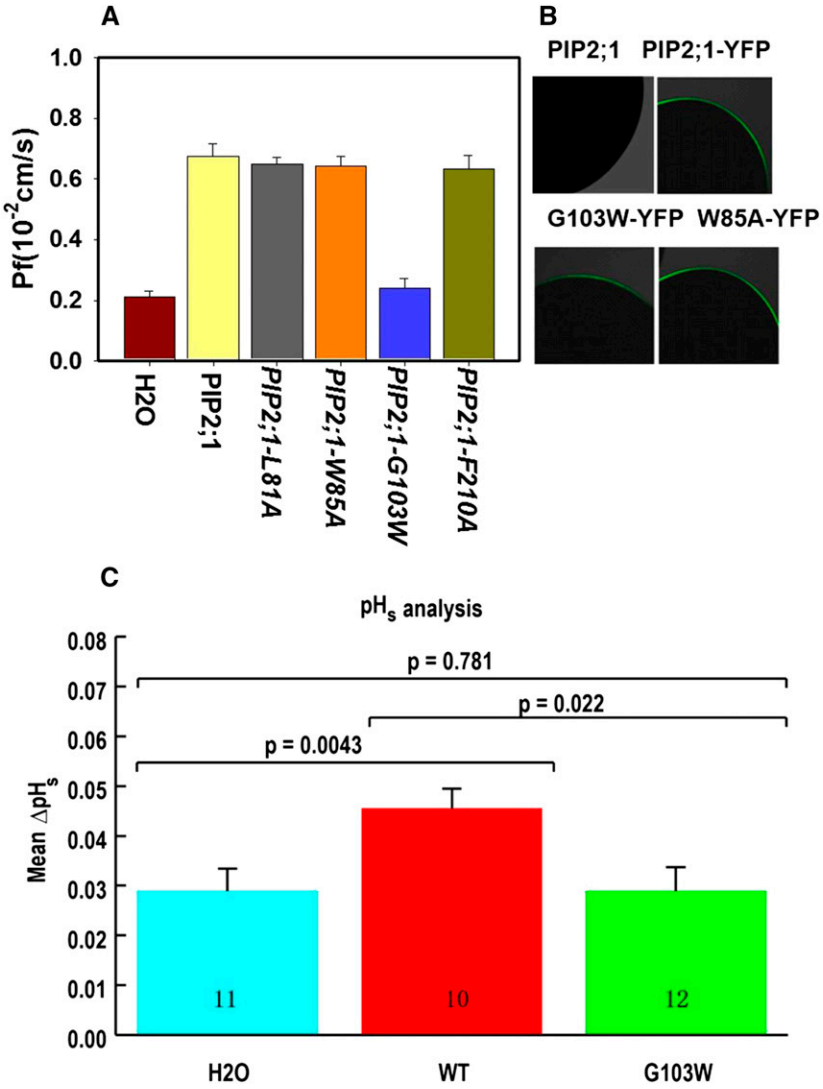

Figure 5. Osmotic Water Permeability Coefficient, PIP2;1 Location in *X. laevis* Oocytes, and Surface pH Analyses.

(A) *PIP2;1-G103W*- and non-PIP2;1-expressing control water-injected oocytes showed a low water permeability. Results are shown as means ± SE measurements from five to eight oocytes from one batch of oocytes.

(B) PIP2;1 and its point mutation isoforms as YFP fusions were present in the vicinity of the oocyte plasma membrane. PIP2;1 alone served as a negative control.

(C) *PIP2;1-G103W* impaired the CO_2 permeability of PIP2;1 as measured by changes in pH_s. The number of oocytes recorded in the same batch are shown in each bar. Data are mean ± SE.

(Heckwolf et al., 2011). Four barley PIP2 aquaporins were recently shown to display CO_2 permeability in *X. laevis* oocytes (Mori et al., 2014). Expression of At-PIP2;1 resulted in a change in the surface pH of oocytes (Musa-Aziz et al., 2009, 2014), showing that Arabidopsis PIP2;1 is permeable to CO_2. Expression of At-βCA4 alone in oocytes also increased the CO_2 permeability (Figure 3E), consistent with maintenance of a CO_2 gradient into oocytes and with previous findings when human α-carbonic anhydrase II was expressed in oocytes (Musa-Aziz et al., 2014).

During the completion phase of this study the RHC1 MATE transporter was identified and reported to function as a candidate bicarbonate sensor based on intracellular HCO_3^- enhancement of SLAC1/OST1/RHC1/HT1-mediated anion channel currents in *X. laevis* oocytes (Tian et al., 2015). Whether SLAC1/OST1 coexpression alone also enables HCO_3^- enhancement of SLAC1-mediated currents and whether RHC1 alone produces an electrogenic current were not investigated in that recent study. In this study, we focused on whether (1) high intracellular HCO_3^- can enhance S-type anion channel currents in *X. laevis* oocytes, (2) on whether we could reconstitute extracellular CO_2/HCO_3^- regulation of SLAC1-mediated anion currents, and (3) on whether we could identify a candidate HCO_3^--responsive protein.

Our experiments show that RHC1 expression alone mediates a clear ionic current in *X. laevis* oocytes that is not dependent on HCO_3^- injection or OST1 coexpression. These findings are

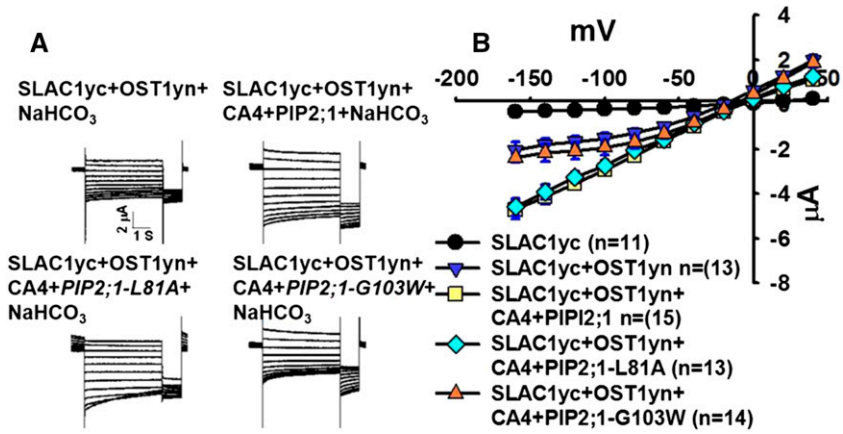

Figure 6. The *PIP2;1-G103W* Mutant Disrupts Extracellular CO_2/HCO_3^--Induced PIP2;1-βCA4 Enhancement of SLAC1/OST1-Mediated Anion Channel Currents in Oocytes.

(A) Whole-cell currents were recorded from oocytes expressing the indicated cRNAs with 11.5 mM $NaHCO_3$ in the bath solution. The voltage protocol was the same as in Figure 1.

(B) Steady state current-voltage relationships from oocytes recorded as in **(A)**. Data are mean ± SE. Results from three independent experiments showed similar results.

consistent with other plant MATE transporters that upon expression produce anion currents in *X. laevis* oocytes (Maron et al., 2010; Melo et al., 2013). Our experiments do not exclude a role for RHC1 in CO_2 signaling (Tian et al., 2015) but point to the need to investigate whether previous findings might result at least in part from additive currents mediated by SLAC1 and RHC1.

Intracellular bicarbonate enhances S-type anion channel currents in wild-type Arabidopsis guard cells (Hu et al., 2010; Xue et al., 2011; Tian et al., 2015). To mimic this process, we coexpressed SLAC1/OST1, SLAC1/CPK6, or SLAC1/CPK23 in *X. laevis* oocytes. We then microinjected $NaHCO_3$ into oocytes at the same concentrations that enhance S-type anion channel currents in guard cells (Hu et al., 2010; Xue et al., 2011; Tian et al., 2015). We found that high intracellular HCO_3^- could enhance SLAC1yc/OST1yn, SLAC1/CPK6, and SLAC1/CPK23-mediated anion channel currents in *X. laevis* oocytes. As the common protein in these analyses is SLAC1, these findings implicate SLAC1 as a candidate CO_2/HCO_3^- sensing protein.

Our findings show that enhancement of SLAC1 activity by intracellular CO_2/HCO_3^- requires the presence of protein kinases (Figure 1). These findings are consistent with the requirements of protein kinase-mediated phosphorylation for activation of SLAC1 (Geiger et al., 2009, 2010; Lee et al., 2009; Brandt et al., 2012; Hua et al., 2012) and the requirement of the OST1 protein kinase for CO_2 signal transduction in plants (Xue et al., 2011; Merilo et al., 2013).

More Than One CO_2/HCO_3^- Sensing Pathway in Guard Cells

Note that our findings do not exclude and indeed support the possibility of more than one CO_2/HCO_3^- sensing mechanism in guard cells, as present and previous findings show the need for protein kinases for CO_2 signal transduction to proceed (Xue et al., 2011; Merilo et al., 2013).

Furthermore, our research shows that while $NaHCO_3$ enhances the activity of SLAC1, significant SLAC1 activity prevails in the absence of exogenous $NaHCO_3$ addition. Thus, a second CO_2/HCO_3^- stimulated pathway would be predicted in guard cells that mediates activation of protein kinases that phosphorylate and activate SLAC1 (Geiger et al., 2009, 2010; Lee et al., 2009; Brandt et al., 2012; Hua et al., 2012; Tian et al., 2015). This hypothesis is supported by a recent study and modeling together suggesting that two distinct CO_2 signal transduction components exist in guard cells, one mediated by the plasma membrane-located βCA4 and one dependent on the chloroplast-targeted βCA1 (Hu et al., 2015). A recent study has shown that the central 10 transmembrane (TM) spans of SLAC1, but not the N and C termini of SLAC1, are required for CO_2 activation of S-type anion channels and CO_2-induced stomatal closing (Yamamoto et al., 2016), in contrast to ABA signaling (Geiger et al., 2009; Lee et al., 2009; Brandt et al., 2015; Yamamoto et al., 2016). These data suggest that that CO_2/HCO_3^- may target the central 10 TM region of SLAC1 and that new phosphorylation sites in this 10 TM region may contribute to SLAC1 activation (Yamamoto et al., 2016). Taken together, we propose that the direct HCO_3^- regulation of SLAC1 found here functions in CO_2 signaling and is not the only bicarbonate-responsive protein in guard cells that contributes to CO_2-induced stomatal closing.

Research has shown that ABA amplifies CO_2-induced stomatal closing (Raschke, 1975; Webb and Hetherington, 1997; Chater et al., 2015; Merilo et al., 2015). A recent study presented findings that were consistent with two nonmutually exclusive possible models: (1) "in which ABA increases the sensitivity of the system to $[CO_2]$" and (2) in which findings "could also be explained by requirement for a CO_2-induced increase in ABA biosynthesis specifically in the guard cell lineage" (Chater et al., 2015). Recent research and this study are consistent with the first model that ABA would be required to enhance parallel CO_2 signaling in mediating stomatal closing (Yamamoto et al., 2016). Further research using ABA nanosensors (Jones et al., 2014b; Waadt et al., 2014) could investigate the second model that CO_2 may also rapidly increase the

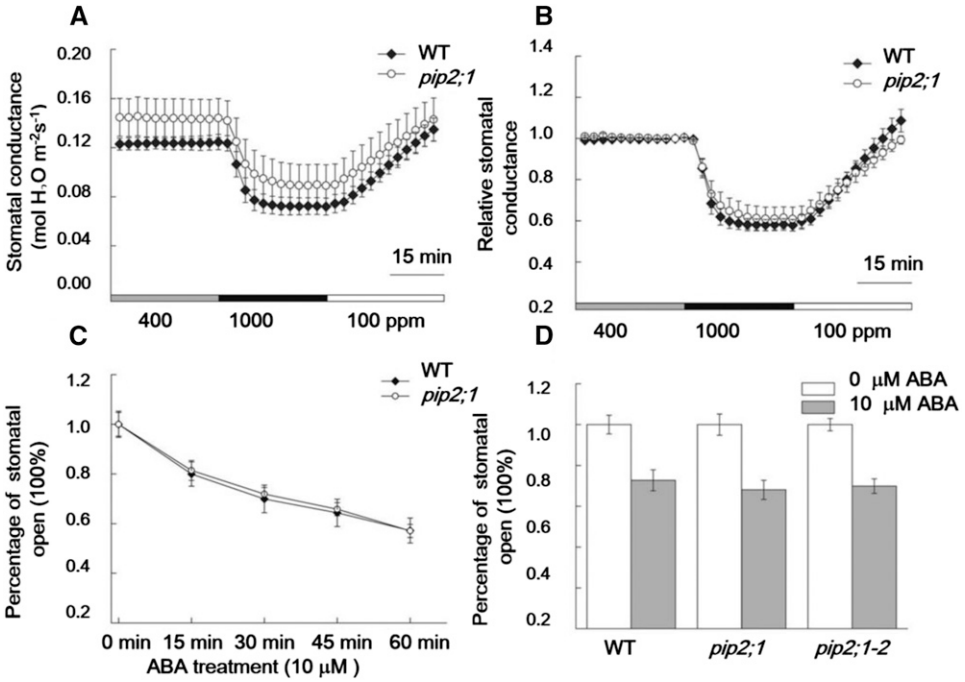

Figure 7. *PIP2;1* Mutation Alone Did Not Significantly Impair CO_2 and ABA Regulation of Stomatal Movements.

(A) Time-resolved intact leaf stomatal conductance in *pip2;1* (CS320492) and wild-type Col plants with [CO_2] shifts indicated at the bottom.
(B) Relative stomatal conductance data shown in **(A)**.
(C) Time-course analysis of stomatal movements in response to ABA treatment in individual mapped stomata in the wild type and *pip2;1* mutant. For these analyses, individual stomata were imaged and tracked (Xue et al., 2011).
(D) Stomatal ABA responses were analyzed in two different *pip2;1* alleles. $n = 3$ experiments, 30 stomata per experiment and condition, genotype blind. Data are mean ± SE.

ABA concentration in guard cells, which cannot be excluded at this time (Chater et al., 2015). In summary, this article and several recent independent studies point to a model in which more than one CO_2 signal transduction pathway in guard cells converge to mediate CO_2-induced stomatal closing, via direct regulation of SLAC1 as found here and via a protein kinase-dependent pathway (Xue et al., 2011; Merilo et al., 2013, 2015; Chater et al., 2015; Hu et al., 2015; Yamamoto et al., 2016).

PIP2;1 and βCA4 Are Required for Reconstitution of Extracellular CO_2/HCO_3^- Regulation

Guard cell transcriptome studies have shown that multiple *PIP2* and *PIP1* aquaporin genes are expressed in guard cells under all investigated conditions (Leonhardt et al., 2004; Yang et al., 2008; Zhao et al., 2008; Bauer et al., 2013). These findings support the hypothesis that higher order mutants in *PIP* aquaporin genes may be needed to affect stomatal CO_2 responses. These findings also are consistent with our results that *pip2;1* T-DNA insertion mutants alone are not sufficient to clearly impair CO_2- and ABA-induced stomatal closing responses (Figure 7). Nevertheless, given that PIP2 aquaporins are both CO_2 and water permeable (Figures 3E and 5; Supplemental Figure 3) (Shelden et al., 2009; Mori et al., 2014), we hypothesize that PIP2;1 functions in both water transport and CO_2 transport in guard cells. Further research with higher order *pip* mutants in the many guard cell-expressed plasma membrane aquaporins (Leonhardt et al., 2004; Yang et al., 2008; Zhao et al., 2008; Bauer et al., 2013) will be needed to investigate this hypothesis.

When βCA4 and PIP2;1 together with SLAC1yc/OST1yn were coexpressed in *X. laevis* oocytes, SLAC1 anion channel currents were enhanced in the presence of extracellular $NaHCO_3$. By contrast, a nonfunctional PIP2;1 point mutant was identified here, PIP2;1-G103W. PIP2;1-G103W was targeted to the plasma membrane of oocytes but did not enable extracellular $NaHCO_3$-dependent enhancement of SLAC1 anion channel currents in *X. laevis* oocytes. The nonfunctional PIP2;1 point mutant PIP2;1-G103W has a mutation analogous to a mutation previously predicted to impair function of the grapevine PIP2;5 aquaporin (Shelden et al., 2009). Two models have been considered for the structural pathway by which CO_2 is transported by aquaporins: (1) CO_2 may be transported via a central pore formed by an aquaporin tetramer. (2) An alternative model has been considered in which CO_2 is transported via the same channel pore as water in each aquaporin subunit (Wang et al., 2007; Horsefield et al., 2008). In this study, the *PIP2;1-G103W* mutation disrupted both water and CO_2 transport, which might be interpreted to support a common pore model for water and CO_2 transport. However, more in depth studies would be needed to fully investigate these two models, as one mutation is insufficient to make a strong conclusion.

The extracellular CO_2/HCO_3^- enhancement of SLAC1yc/OST1yn-mediated anion channel currents by βCA4 and PIP2;1

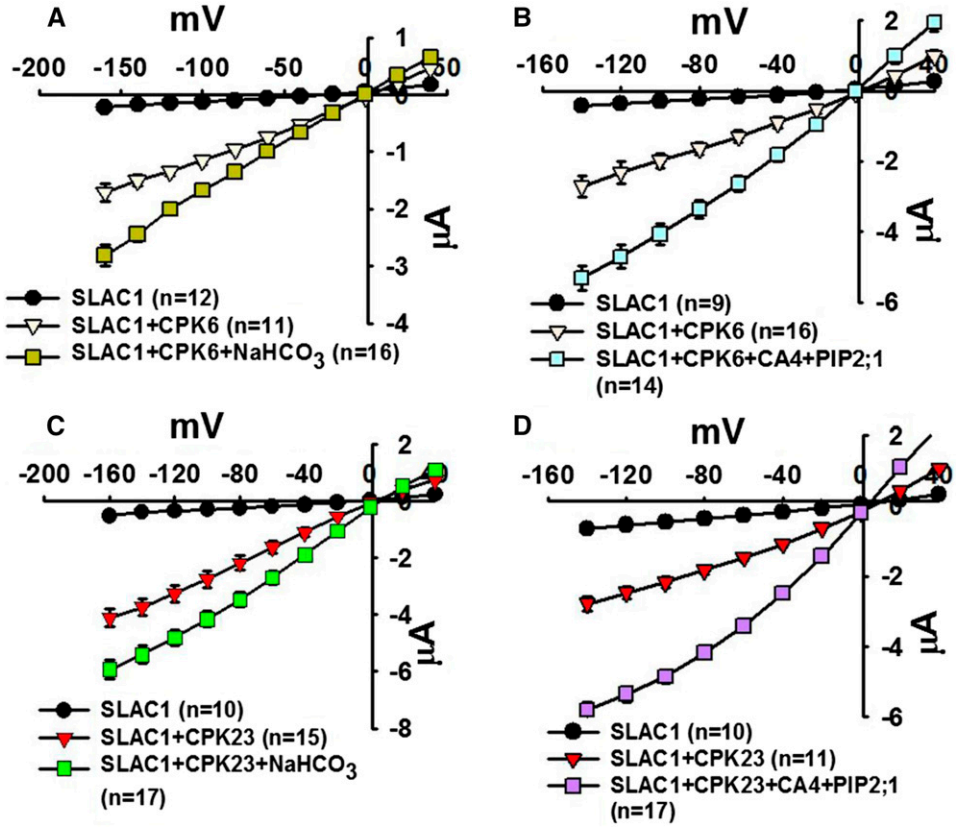

Figure 8. Intracellular Bicarbonate Enhances Currents Mediated by the SLAC1 Anion Channel in CPK6-SLAC1- or CPK23-SLAC1-Expressing Oocytes and Extracellular Bicarbonate Enhances Currents in βCA4, PIP2;1, and CPK6-SLAC1- or CPK23-SLAC1-Coexpressing oocytes.

(A) and **(C)** Bicarbonate injection into oocytes enhanced SLAC1 anion channel currents when SLAC1 was coexpressed with the Ca^{2+}-dependent protein kinases CPK6 or CPK23 rather than OST1 in oocytes.

(B) and **(D)** βCA4 and PIP2;1 coexpression with 11.5 mM $NaHCO_3$ in the bath solution enhanced SLAC1/CPK6- and SLAC1/CPK23-mediated anion channel currents. Data are mean ± SE. Results from four independent batches of oocytes showed similar results.

requires functional PIP2;1. We were able to reconstitute extracellular CO_2/HCO_3^- regulation of SLAC1-mediated anion currents in *X. laevis* oocytes by coexpression of βCA4, PIP2;1, SLAC1, and either OST1, CPK6, or CPK23. We propose the following working model for mechanisms contributing to the CO_2 signaling pathway that results in stomatal closure. When the CO_2 concentration in leaves (*Ci*) is elevated, CO_2 influx across the plasma membrane of guard cells is enhanced through aquaporins. The carbonic anhydrases accelerate the production of intracellular HCO_3^-, and elevated intracellular CO_2/HCO_3^- enhances SLAC1 anion channel activity, contributing to the closure of stomatal pores. When *Ci* is low, as occurs during the light phase (Hanstein et al., 2001), the intracellular CO_2/HCO_3^- concentration is reduced and S-type anion channel activity is reduced.

METHODS

Two-Electrode Voltage-Clamp Recordings in *Xenopus laevis* Oocytes

cDNA constructs, CA4 amplified by CA4NBF/CA4NBR, PIP2;1 amplified by PIP2A-pNB1F/PIP2A-pNB1R, SIP1 amplified by SIP1A-pNB1F/SIP1A-pNB1R, and RHC1 amplified by RHC1-pNB1F/RHC1-pNB1R were cloned into the pNB1 vector for expression in oocytes using the USER method (Nour-Eldin et al., 2006). All primers are listed in Supplemental Table 1. cRNAs were synthesized from 0.5 to 1 μg of linearized plasmid DNA template using the mMessage mMachine in vitro transcription kit (Ambion). Approximately 20 ng of each indicated cRNA was injected into oocytes for voltage-clamp recordings; 5 ng was used for PIP2;1 and CA4 cRNA. Injected oocytes were incubated in ND96 buffer at 16°C for 2 to 3 d prior to electrophysiological recording. The ND96 buffer contained 10 mM MES/Tris (pH 7.5), 1 mM $CaCl_2$, 1 mM $MgCl_2$, and 96 mM NaCl. Whole-cell ionic currents were recorded with a Cornerstone (Dagan) TEV-200 two-electrode voltage-clamp amplifier and digitized using an Axon Instruments Digidata 1440A low-noise data acquisition system (Molecular Devices) controlled by pClamp acquisition software (Molecular Devices). Microelectrodes were fabricated with a P-87 Flaming/Brown microelectrode micropipette puller (Sutter) from borosilicate glass (GC200TF-10; Warner Instruments) and the tips were filled with 3 M KCl. The resistance of the filled electrodes was 0.5 to 1.5 MΩ.

As oocyte batches vary in the protein expression level among batches and, thus, the magnitude of ionic currents from one week to another varies, the indicated controls were included in each batch of oocytes and control conditions were recorded intermittently with investigated conditions to avoid time-of-measurement dependence in the data. Furthermore, data from one representative batch of oocytes are shown with controls in each

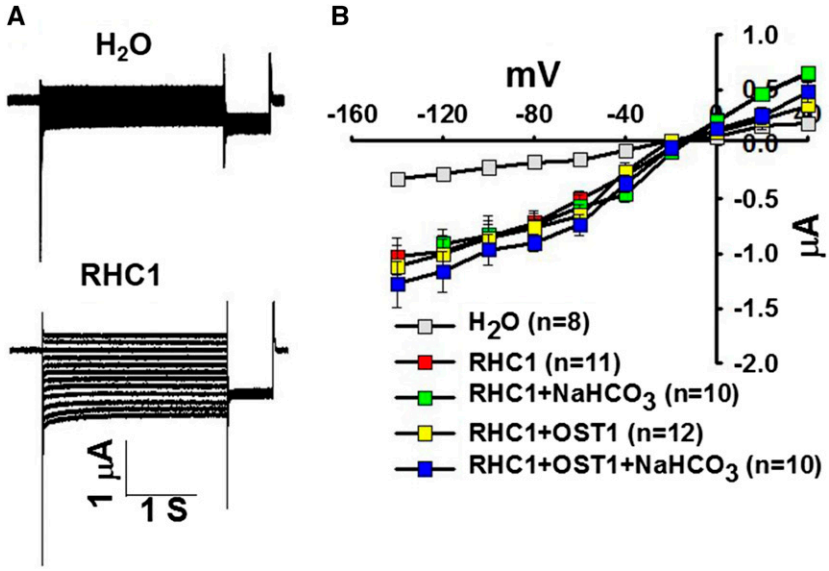

Figure 9. RHC1 Expression in Oocytes Causes Ionic Currents and Intracellular Bicarbonate Does Not Enhance RHC1-Mediated Anion Channel Currents in *X. laevis* Oocytes in the Presence or Absence of the Protein Kinase OST1.

(A) Whole-cell currents were recorded from oocytes expressing the indicated cRNAs.
(B) Steady state current-voltage relationships from oocytes recorded as in **(A)**. Due to overlapping data of "RHC1" and "RHC1+$NaHCO_3$," alternating data points are shown. Data are mean ± SE. Results from three independent experiments showed similar results.

figure and were reproduced in at least three independent oocyte batches as indicated. The numbers of oocytes recorded for each condition in the depicted batch of oocytes are also provided in the figures. Oocytes were recorded in 10 mM MES/Tris (pH 7.4), 1 mM $MgCl_2$, 1 mM $CaCl_2$, 2 mM KCl, 24 mM NaCl, and 70 mM Na-gluconate buffer. Osmolality was adjusted to 220 mM using D-sorbitol. In Supplemental Figure 1B, 2 mM KCl, 24 mM NaCl, and 70 mM Na-gluconate were replaced by 96 mM NaCl. Steady state currents were recorded starting from a holding potential of 0 mV and ranging from +40 to −160 mV in −20-mV decrements, followed by a −120-mV voltage "tail" pulse. Note that the time-dependent properties of SLAC1 channel in *Xenopus laevis* oocytes vary among individual oocytes. This variability in time-dependent properties was noted in early studies of S-type anion channel currents in guard cells (Schmidt and Schroeder, 1994) and may depend on posttranslational modification of the channel protein that requires further analyses. The data acquisition rate in these electrophysiological experiments was 20 kHz, and data were low-pass filtered at 500 Hz. For application of intracellular bicarbonate, $NaHCO_3$ was injected into each oocyte and the final concentration is given in the figure legends. The concentrations of free bicarbonate and CO_2 were calculated using the Henderson-Hasselbalch equation ($pH = pK_1 + \log [HCO_3^-]/[CO_2]$), where $[HCO_3^-]$ represents the free bicarbonate concentration and $[CO_2]$ represents the free CO_2 concentration; $pK_1 = 6.352$ was used for the calculation (Speight, 2005). Injection of 11.5 mM $NaHCO_3$ results in 10.5 mM free HCO_3^- and 1 mM free CO_2 at pH 7.4. The calculation of intracellular bicarbonate was based on cytosolic oocyte volumes approximately equal to 500 nL, and the volume of injected $NaHCO_3$ buffer was 50 nL. Bicarbonate microinjections were performed 20 min before voltage-clamp experiments. All experiments were performed at room temperature. Surface pH measurements and the water swelling assay in *X. laevis* oocytes were performed as described (Geyer et al., 2013; Musa-Aziz et al., 2014). Briefly, a baked, silanized [*bis*-di-(methylamino)-dimethylsilane; Sigma-Aldrich] borosilicate glass microelectrode, with a H^+ Ionophore I liquid membrane (mixture B; Sigma-Aldrich) at its 15-μm (i.d.) tip, and backfilled with a solution (containing, in mM, 40 KH_2PO_4, 23 NaOH, and 15 NaCl, adjusted to pH 7.0) was used to measure pH_s. The pH_s microelectrode was connected to a FD223 electrometer (World Precision Instruments) and mounted on an ultrafine micromanipulator (model MPC-200 system; Sutter Instrument Co.) to position the pH_s electrode tip at the surface of the oocyte. To record pH_s, the tip was then advanced a further ~40 μm, creating a visible dimple on the oocyte membrane. Periodically the electrode tip was withdrawn ~300 μm for recalibration in the bulk extracellular fluid (pH 7.50). Composition of ND96 and 5% CO_2/33 mM HCO_3^- solutions were as described by Musa-Aziz et al. (2014) and flowed into the chamber at 4 mL/min.

Confocal Microscopy

Confocal imaging of PIP2;1-YFP fusion proteins expressed in *X. laevis* oocytes was acquired by spinning-disc confocal microscopy (Nikon Eclipse TE2000-U). Images show an optical slice of each oocyte. Fluorescence microscopy images were obtained with an EMCCD camera (Cascade II 512; Photometrics) and analyzed with Metamorph software (Universal Imaging).

Yeast Two-Hybrid Screen

For isolation of βCA4-interacting proteins, a yeast two-hybrid screen was conducted. For isolation of βCA4-interacting proteins, a yeast two-hybrid screen was conducted. βCA4 amplified by primers of CA4GBKF/CA4GBKR was digested by *Eco*RI/*Kpn*I and ligated with GAL4-BD in the vector pGBKT7 (Causier and Davies, 2002). pGBKT7-βCA4 was used as bait to screen for interacting proteins from a normalized commercial *Arabidopsis thaliana* cDNA library constructed in the pGADT7 vector (Clontech). pGBKT7-βCA4 was transformed into the yeast strain Y2HGold and the library was in the Y187 strain. The mating method was adopted, and diploid cells were grown on the SD-Leu-Trp medium plus 40 mg/mL X-Gal at pH 5.8. Interactions were detected as blue cells, but no robust yeast two-hybrid interactors of *βCA4* were identified in this screen.

SUS Analyses

The SUS was adopted and improved to test direct protein-protein interactions and to screen βCA-interacting proteins from an Arabidopsis cDNA library (Grefen et al., 2007). The βCA4 cDNA amplified by CA4F/CA4R was cloned into the vector pMetYC-DEST (Grefen et al., 2007) by Gateway recombination. pMetYC-βCA4 was used as a bait to screen an Arabidopsis cDNA library, which was constructed in the prey vector pNX33-DEST (Grefen et al., 2007). pMetYC-βCA4 was used as a bait to screen an Arabidopsis cDNA library, which was constructed in the prey vector pNX33-DEST. The THYAP4 yeast colonies transformed with pMetYC-βCA4 were mated with the THYAP5 yeast transformed with 3 μg of the Arabidopsis cDNA library (Grefen et al., 2007). The cotransformants were grown on SD-Leu-Trp medium plus 40 mg/mL X-Gal at pH 5.8. Blue colonies indicated putative interactions.

BiFC Experiments in *Nicotiana benthamiana*

For split YFP complementation assays (BiFC), the vectors pXCSG-YN155 and pXCSG-YC84 were used. To generate the βCA4-YC84 and PIP2;1-YN155 constructs, full-length PIP2;1 cDNA amplified by PIP2AF/PIP2AR was amplified and cloned into the binary vector pXCSG-YN155, and βCA4 cDNA amplified by CA4F/CA4R was amplified and cloned as a fusion with the binary vector pXCSG-YC84 by Gateway recombination. Split luciferase assays were performed as described (Chen et al., 2008). Briefly, the *PIP2;1* cDNA was cloned into a vector containing the C-terminal half of luciferase (cLUC) and *βCA4* was cloned into the N-terminal half of luciferase (nLUC). These constructs were transformed into the *Agrobacterium tumefaciens* strain GV3101 and then coinfiltrated into *N. benthamiana* leaves with P19 at an OD_{600} of 0.8. After 3 d of infiltration, the infiltrated leaves were harvested for bioluminescence detection. Images were captured with a CCD camera.

Coimmunoprecipitation Experiments in *N. benthamiana*

The Agrobacterium strain GV3101 with the helper plasmid pMP90K carrying βCA4 and PIP2;1 was coinfiltrated at an OD_{600} of 0.8 with the p19 strain in *N. benthamiana*. Protein extraction was performed with infiltrated leaves 3 d after infiltration (Nishimura et al., 2010). Infiltrated leaves were then sprayed with water containing 0.01% Silwet L-77 after 3 d infiltration before leaf excision. Leaf samples (1.0 g) were ground in liquid nitrogen, and the powdered tissues were suspended in 2 mL of extraction buffer (50 mM Na-phosphate, pH 7.4, 1 mM DTT, 0.1% Nonidet P-40, 150 mM NaCl, and 1× protease inhibitor cocktail). Crude extracts were centrifuged at 18,000*g* for 20 min at 4°C. Supernatant passed through Miracloth (Calbiochem) was used as an input for immunoprecipitation. Input proteins were incubated with 50 μL anti-HA matrix (Roche) for 3 h at 4°C and the immunocomplexes were washed with 500 μL washing buffer four times (50 mM Na-phosphate, 0.1% Nonidet P-40, and 150 mM NaCl, pH 7.4). Proteins were separated by 10% SDS-PAGE gel and electrotransferred onto immobilon-P membrane. Membranes were blocked in PBS-T buffer with 5% skim milk overnight (Bio-Rad) and then washed three times with PBS-T buffer and incubated with anti-GFP (Roche) or anti-HA antibodies.

The membranes were incubated with 1:10,000 diluted anti-mouse horseradish peroxidase-conjugated for 1 h. Bio-Rad's Clarity ECL protein gel blotting substrate was then used to perform detection.

Time-Resolved Intact Leaf Stomatal Conductance Experiments

Four- to six-week-old Col-0 and *pip2;1* plants growing in a growth chamber at 70% humidity (70 $\mu mol\ m^{-2}\ s^{-1}$ light intensity, 21°C, 16 h light/8 h dark) were used for intact-leaf CO_2-induced stomatal conductance change analyses as previously described (Hu et al., 2010). Briefly, stomatal conductance was first stabilized at 400 ppm [CO_2] and recorded for an additional 30 min and then [CO_2] was shifted to elevated CO_2 for 30 min and then again changed to 100 ppm. Data are means of four leaves per genotype per treatment ± SE. Relative stomatal conductance values were determined by averaging 10 data points at 400 ppm [CO_2] preceding the [CO_2] elevation for normalization.

Stomatal Aperture Measurements

Three-week-old Arabidopsis plants including Col-0, *pip2;1*, and *pip2;1-2* grown in a growth chamber at 70% humidity were used for analyses of stomatal movements in response to ABA. qPCR analyses suggested that *pip2;1* is a knockdown mutant. Expression levels were compared with that of *EF-1a* assessed using qEF-1aF/qEF-1aR. qPCR analyses suggest that *pip2;1-2* (Grondin et al., 2015) is a knockdown mutant. Expression was compared with *EF-1a*. qRT-PCR was performed using a Bio-Rad CFX96 touch under the following conditions: 95°C for 2 min; 40 cycles of 95°C for 15 s, 60°C for 15 s, and 72°C for 20 s. Intact leaf epidermal layers with no mesophyll cells in the vicinity were prepared as described (Hu et al., 2010; Xue et al., 2011). Leaf epidermal layers were preincubated for 2 h in opening buffer (10 mM MES, 10 mM KCl, and 50 μM $CaCl_2$ at pH 6.15) and then incubated with buffers supplemented with 10 μM ABA. For time-course analyses, individual stomata were imaged and individually tracked at different time points. Stomatal apertures were measured using ImageJ (Schneider et al., 2012). Data from genotype-blind analyses are shown (n = 3 experiments, 30 stomata per experiment and condition).

Simulation of CO_2 Transport in Oocytes

Our model describes the dynamics of CO_2 influx using a set of differential equations and is detailed in previous work (Somersalo et al., 2012). Briefly, it consists of a spherical oocyte of radius 650 μm surrounded by a layer of unconvected extracellular fluid of thickness d = 100 μm in which reactions can take place. The oocyte and fluid layer are immersed in a bath in which the concentrations of the reactants are assumed to be constant. Within the layer and the oocyte, the model describes the formation and disassociation of carbonic acid as:

$$CO_2 + H_2O \underset{k_{-1}}{\overset{k_1}{\rightleftharpoons}} H_2CO_3 \underset{k_{-2}}{\overset{k_2}{\rightleftharpoons}} HCO_3^- + H^+$$

where k_1, k_{-1}, k_2, and k_{-2} are rate constants. In addition, we assumed that there is one non-CO_2/HCO_3^- buffer, denoted by HA/A^-.

$$HA \underset{k_{-3}}{\overset{k_3}{\rightleftharpoons}} A^- + H^+$$

We assumed that the membrane is permeable to CO_2 and incorporated intracellular carbonic anhydrase-like activity by multiplying the rate constants k_1 and k_{-1} by an acceleration factor F. Assuming spherical symmetry, the rate equations corresponding to the above reactions can be solved along a radial line using the methods-of-line algorithm. All parameters and initial conditions were chosen as in the study by Somersalo et al. (2012) with the exception of the membrane permeability $P_{M\,CO2}$, which was chosen to be lower.

Accession Numbers

Sequence data from this article can be found in the Arabidopsis Genome Initiative or GenBank/EMBL databases under the following accession numbers: SLAC1 (AT1G12480), OST1 (AT4G33950), CA4 (AT1G70410), PIP2;1 (AT3G53420), CPK6 (AT2G17290), CPK23 (AT4G04740), RHC1 (AT4G22790), and SIP1A (At3g04090).

Supplemental Data

Supplemental Figure 1. Injection of 11.5 mM $NaHCO_3$ at pH 7.0 or pH 8.0 into oocytes and recordings in 96 mM NaCl extracellular buffer also cause enhancement of SLAC1-mediated anion channel currents, whereas 23 mM sorbitol injection has no effect on SLAC1 activity.

Supplemental Figure 2. Steady state current-voltage relationships show the average magnitude of SLAC1yc/OST1yn-mediated anion channel currents recorded from oocytes injected with 11.5 mM NaCl were reduced rather than enhanced.

Supplemental Figure 3. Surface pH (pH_s) measurements from oocytes exposed to CO_2/HCO_3^-.

Supplemental Figure 4. The *PIP2;1-W85A* and *PIP2;1-F210A* mutation isoforms do not impair the PIP2;1-CA4 enhancement of SLAC1/OST1-mediated anion channel currents in oocytes by extracellular CO_2/HCO_3^-.

Supplemental Figure 5. Simulated membrane surface pH (pH_s) as a function of time for baseline parameter values, in the presence of intracellular carbonic anhydrase (CA) activity, for simulated increased membrane CO_2 permeability, and in the presence of both intracellular CA activity and increased membrane CO_2 permeability.

Supplemental Figure 6. Structure of *PIP2;1* gene and T-DNA insertion; qPCR analyses suggested that *pip2;1* is a knockdown mutant; qPCR analyses suggest that *pip2;1-2* is a knockdown mutant.

Supplemental Table 1. Primers used for construct and expression studies.

ACKNOWLEDGMENTS

We thank Aaron Stephan (University of California San Diego), Benjamin Brandt (University of Geneva), and Fraser Moss (Case Western Reserve University) for comments on the manuscript. We thank Steve Tyerman (University of Adelaide) for suggesting the test of the PIP2;1 G103W mutation based on Shelden et al. (2009) and Anton Schäffner (Helmholtz Zentrum Munich) for providing Arabidopsis mutant line *pip2;1-2*. We thank Cawas Engineer for providing the graphic icon. This research was funded by a grant from the National Science Foundation (MCB1414339) to J.I.S. and W.-J.R. and in part supported by grants from the National Institutes of Health (GM060396-ES010337) to J.I.S. and the China National Natural Science Foundation (31271515), the Fundamental Research Funds for the Central Universities (2662015PY179), and the "1000-talents Plan" for young researchers from China to H.H. Surface pH experiments were supported by American Heart Association Postdoctoral Fellowships (AHA09POST2060873 and AHA11POST7670014) to X.Q. and Office of Naval Research Grants (N00014-11-1-0889, N00014-14-1-0716, and N00014-15-1-2060), the National Institutes of Health (U01-GM111251), and the Meyer/Scarpa Chair to W.F.B.

AUTHOR CONTRIBUTIONS

C.W. performed all of the oocyte two-electrode voltage clamp electrophysiological experiments and data analyses. H.H. performed SUS, BiFC, and coimmunoprecipitation experiments at UCSD. X.Q. and B.Z. performed surface pH experiments. C.W., X.Q., and B.Z. performed osmotic water permeability measurements on *X. laevis* oocytes. D.X. performed split luciferase experiments as well as ABA- and CO_2-induced stomatal movement assays in *PIP2;1* mutants. W.-J.R. constructed the mathematical model and performed simulations. J.I.S. conceived the project. C.W., H.H., W.F.B., W.-J.R., and J.I.S. contributed to the research design and provided support and suggestions throughout the research and manuscript preparation. C.W. and J.I.S. wrote the manuscript with contributions from other authors.

Received July 17, 2015; revised December 18, 2015; accepted January 11, 2016; published January 13, 2016.

REFERENCES

Ainsworth, E.A., and Long, S.P. (2005). What have we learned from 15 years of free-air CO_2 enrichment (FACE)? A meta-analytic review of the responses of photosynthesis, canopy properties and plant production to rising CO_2. New Phytol. **165:** 351–371.

Battisti, D.S., and Naylor, R.L. (2009). Historical warnings of future food insecurity with unprecedented seasonal heat. Science **323:** 240–244.

Bauer, H., et al. (2013). The stomatal response to reduced relative humidity requires guard cell-autonomous ABA synthesis. Curr. Biol. **23:** 53–57.

Bracha-Drori, K., Shichrur, K., Katz, A., Oliva, M., Angelovici, R., Yalovsky, S., and Ohad, N. (2004). Detection of protein-protein interactions in plants using bimolecular fluorescence complementation. Plant J. **40:** 419–427.

Brandt, B., Brodsky, D.E., Xue, S., Negi, J., Iba, K., Kangasjärvi, J., Ghassemian, M., Stephan, A.B., Hu, H., and Schroeder, J.I. (2012). Reconstitution of abscisic acid activation of SLAC1 anion channel by CPK6 and OST1 kinases and branched ABI1 PP2C phosphatase action. Proc. Natl. Acad. Sci. USA **109:** 10593–10598.

Brandt, B., Munemasa, S., Wang, C., Nguyen, D., Yong, T., and Yang, P.G., Poretsky, E., Belknap, T.F., Waadt, R., Alemán, F., and Schroeder, J. (2015). Calcium specificity signaling mechanisms in abscisic acid signal transduction in Arabidopsis guard cells. eLife **4:** e03599.

Causier, B., and Davies, B. (2002). Analysing protein-protein interactions with the yeast two-hybrid system. Plant Mol. Biol. **50:** 855–870.

Chater, C., et al. (2015). Elevated CO_2-induced responses in stomata require ABA and ABA signaling. Curr. Biol. **25:** 2709–2716.

Chen, H., Zou, Y., Shang, Y., Lin, H., Wang, Y., Cai, R., Tang, X., and Zhou, J.M. (2008). Firefly luciferase complementation imaging assay for protein-protein interactions in plants. Plant Physiol. **146:** 368–376.

Da Ines, O., Graf, W., Franck, K.I., Albert, A., Winkler, J.B., Scherb, H., Stichler, W., and Schäffner, A.R. (2010). Kinetic analyses of plant water relocation using deuterium as tracer - reduced water flux of *Arabidopsis pip2* aquaporin knockout mutants. Plant Biol. (Stuttg.) **12** (suppl. 1): 129–139.

Fabre, N., Reiter, I.M., Becuwe-Linka, N., Genty, B., and Rumeau, D. (2007). Characterization and expression analysis of genes encoding alpha and beta carbonic anhydrases in Arabidopsis. Plant Cell Environ. **30:** 617–629.

Frommer, W.B. (2010). Biochemistry. CO_2mmon sense. Science **327:** 275–276.

Fujiyoshi, Y., Mitsuoka, K., de Groot, B.L., Philippsen, A., Grubmüller, H., Agre, P., and Engel, A. (2002). Structure and function of water channels. Curr. Opin. Struct. Biol. **12:** 509–515.

Geiger, D., Scherzer, S., Mumm, P., Marten, I., Ache, P., Matschi, S., Liese, A., Wellmann, C., Al-Rasheid, K.A., Grill, E., Romeis, T., and Hedrich, R. (2010). Guard cell anion channel SLAC1 is regulated by CDPK protein kinases with distinct Ca^{2+} affinities. Proc. Natl. Acad. Sci. USA **107:** 8023–8028.

Geiger, D., Scherzer, S., Mumm, P., Stange, A., Marten, I., Bauer, H., Ache, P., Matschi, S., Liese, A., Al-Rasheid, K.A., Romeis, T., and Hedrich, R. (2009). Activity of guard cell anion channel SLAC1 is controlled by drought-stress signaling kinase-phosphatase pair. Proc. Natl. Acad. Sci. USA **106:** 21425–21430.

Geyer, R.R., Musa-Aziz, R., Qin, X., and Boron, W.F. (2013). Relative CO(2)/NH(3) selectivities of mammalian aquaporins 0-9. Am. J. Physiol. Cell Physiol. **304:** C985–C994.

Grefen, C., Lalonde, S., and Obrdlik, P. (2007). Split-ubiquitin system for identifying protein-protein interactions in membrane and full-length proteins. Curr. Protoc. Neurosci. **5:** 27.

Grondin, A., Rodrigues, O., Verdoucq, L., Merlot, S., Leonhardt, N., and Maurel, C. (2015). Aquaporins contribute to ABA-triggered stomatal closure through OST1-mediated phosphorylation. Plant Cell **27:** 1945–1954.

Hanstein, S., Beer, D., and Felle, H.H. (2001). Miniaturised carbon dioxide sensor designed for measurements within plant leaves. Sens. Actuators B Chem. **81:** 107–114.

Hashimoto, M., Negi, J., Young, J., Israelsson, M., Schroeder, J.I., and Iba, K. (2006). Arabidopsis HT1 kinase controls stomatal movements in response to CO_2. Nat. Cell Biol. **8:** 391–397.

Heckwolf, M., Pater, D., Hanson, D.T., and Kaldenhoff, R. (2011). The *Arabidopsis thaliana* aquaporin AtPIP1;2 is a physiologically relevant CO_2 transport facilitator. Plant J. **67:** 795–804.

Hetherington, A.M., and Woodward, F.I. (2003). The role of stomata in sensing and driving environmental change. Nature **424:** 901–908.

Holden, C. (2009). Climate change. Higher temperatures seen reducing global harvests. Science **323:** 193.

Horsefield, R., Nordén, K., Fellert, M., Backmark, A., Törnroth-Horsefield, S., Terwisscha van Scheltinga, A.C., Kvassman, J., Kjellbom, P., Johanson, U., and Neutze, R. (2008). High-resolution x-ray structure of human aquaporin 5. Proc. Natl. Acad. Sci. USA **105:** 13327–13332.

Hu, H., Boisson-Dernier, A., Israelsson-Nordström, M., Böhmer, M., Xue, S., Ries, A., Godoski, J., Kuhn, J.M., and Schroeder, J.I. (2010). Carbonic anhydrases are upstream regulators of CO_2-controlled stomatal movements in guard cells. Nat. Cell Biol. **12:** 87–93, 1–18.

Hu, H., Rappel, W.J., Occhipinti, R., Ries, A., Böhmer, M., You, L., Xiao, C., Engineer, C.B., Boron, W.F., and Schroeder, J.I. (2015). Distinct cellular locations of carbonic anhydrases mediate CO_2 control of stomatal, movements. Plant Physiol. **169:** 1168–1178.

Hua, D., Wang, C., He, J., Liao, H., Duan, Y., Zhu, Z., Guo, Y., Chen, Z., and Gong, Z. (2012). A plasma membrane receptor kinase, GHR1, mediates abscisic acid- and hydrogen peroxide-regulated stomatal movement in Arabidopsis. Plant Cell **24:** 2546–2561.

Jones, A.M., et al. (2014a). Border control–a membrane-linked interactome of *Arabidopsis.* Science **344:** 711–716.

Jones, A.M., Danielson, J.A., Manojkumar, S.N., Lanquar, V., Grossmann, G., and Frommer, W.B. (2014b). Abscisic acid dynamics in roots detected with genetically encoded FRET sensors. eLife **3:** e01741.

Kim, T.H., Böhmer, M., Hu, H., Nishimura, N., and Schroeder, J.I. (2010). Guard cell signal transduction network: advances in understanding abscisic acid, CO_2, and Ca^{2+} signaling. Annu. Rev. Plant Biol. **61:** 561–591.

Kukulski, W., Schenk, A.D., Johanson, U., Braun, T., de Groot, B.L., Fotiadis, D., Kjellbom, P., and Engel, A. (2005). The 5A structure of heterologously expressed plant aquaporin SoPIP2;1. J. Mol. Biol. **350:** 611–616.

LaDeau, S.L., and Clark, J.S. (2001). Rising CO_2 levels and the fecundity of forest trees. Science **292:** 95–98.

Lee, S.C., Lan, W., Buchanan, B.B., and Luan, S. (2009). A protein kinase-phosphatase pair interacts with an ion channel to regulate ABA signaling in plant guard cells. Proc. Natl. Acad. Sci. USA **106:** 21419–21424.

Leonhardt, N., Kwak, J.M., Robert, N., Waner, D., Leonhardt, G., and Schroeder, J.I. (2004). Microarray expression analyses of Arabidopsis guard cells and isolation of a recessive abscisic acid hypersensitive protein phosphatase 2C mutant. Plant Cell **16:** 596–615.

Maron, L.G., Piñeros, M.A., Guimarães, C.T., Magalhaes, J.V., Pleiman, J.K., Mao, C., Shaff, J., Belicuas, S.N.J., and Kochian, L.V. (2010). Two functionally distinct members of the MATE (multidrug and toxic compound extrusion) family of transporters potentially underlie two major aluminum tolerance QTLs in maize. Plant J. **61:** 728–740.

Medlyn, B., Barton, C., Broadmeadow, M., Ceulemans, R., De Angelis, P., Forstreuter, M., Freeman, M., Jackson, S., Kellomki, S., and Laitat, E. (2001). Stomatal conductance of forest species after long term exposure to elevated CO_2 concentration: A synthesis. New Phytol. **149:** 247–264.

Melo, J.O., et al. (2013). Incomplete transfer of accessory loci influencing SbMATE expression underlies genetic background effects for aluminum tolerance in sorghum. Plant J. **73:** 276–288.

Merilo, E., Jalakas, P., Kollist, H., and Brosché, M. (2015). The role of ABA recycling and transporter proteins in rapid stomatal responses to reduced air humidity, elevated CO_2, and exogenous ABA. Mol. Plant **8:** 657–659.

Merilo, E., Laanemets, K., Hu, H., Xue, S., Jakobson, L., Tulva, I., Gonzalez-Guzman, M., Rodriguez, P.L., Schroeder, J.I., Broschè, M., and Kollist, H. (2013). PYR/RCAR receptors contribute to ozone-, reduced air humidity-, darkness-, and CO_2-induced stomatal regulation. Plant Physiol. **162:** 1652–1668.

Mori, I.C., Rhee, J., Shibasaka, M., Sasano, S., Kaneko, T., Horie, T., and Katsuhara, M. (2014). CO_2 transport by PIP2 aquaporins of barley. Plant Cell Physiol. **55:** 251–257.

Murata, Y., Mori, I.C., and Munemasa, S. (2015). Diverse stomatal signaling and the signal integration mechanism. Annu. Rev. Plant Biol. **66:** 369–392.

Musa-Aziz, R., Chen, L.-M., Pelletier, M.F., and Boron, W.F. (2009). Relative CO_2/NH_3 selectivities of AQP1, AQP4, AQP5, AmtB, and RhAG. Proc. Natl. Acad. Sci. USA **106:** 5406–5411.

Musa-Aziz, R., Occhipinti, R., and Boron, W.F. (2014). Evidence from simultaneous intracellular- and surface-pH transients that carbonic anhydrase IV enhances CO2 fluxes across Xenopus oocyte plasma membranes. Am. J. Physiol. Cell Physiol. **307:** C814–C840.

Negi, J., Matsuda, O., Nagasawa, T., Oba, Y., Takahashi, H., Kawai-Yamada, M., Uchimiya, H., Hashimoto, M., and Iba, K. (2008). CO_2 regulator SLAC1 and its homologues are essential for anion homeostasis in plant cells. Nature **452:** 483–486.

Nour-Eldin, H.H., Hansen, B.G., Nørholm, M.H., Jensen, J.K., and Halkier, B.A. (2006). Advancing uracil-excision based cloning towards an ideal technique for cloning PCR fragments. Nucleic Acids Res. **34:** e122.

Nyblom, M., Frick, A., Wang, Y., Ekvall, M., Hallgren, K., Hedfalk, K., Neutze, R., Tajkhorshid, E., and Törnroth-Horsefield, S. (2009). Structural and functional analysis of SoPIP2;1 mutants adds insight into plant aquaporin gating. J. Mol. Biol. **387:** 653–668.

Nishimura, N., Sarkeshik, A., Nito, K., Park, S.Y., Wang, A., Carvalho, P.C., Lee, S., Caddell, D.F., Cutler, S.R., Chory, J., Yates, J.R., and Schroeder, J.I. (2010). PYR/PYL/RCAR family members are major in-vivo ABI1 protein phosphatase 2C-interacting proteins in Arabidopsis. Plant J. **61:** 290–299.

Raschke, K. (1975). Simultaneous requirement of carbon dioxide and abscisic acid for stomatal closing in *Xanthium strumarium L.* Planta **125:** 243–259.

Ren, G., Cheng, A., Reddy, V., Melnyk, P., and Mitra, A.K. (2000). Three-dimensional fold of the human AQP1 water channel determined at 4 A resolution by electron crystallography of two-dimensional crystals embedded in ice. J. Mol. Biol. **301:** 369–387.

Roelfsema, M.R., Hedrich, R., and Geiger, D. (2012). Anion channels: master switches of stress responses. Trends Plant Sci. **17:** 221–229.

Schmidt, C., and Schroeder, J.I. (1994). Anion selectivity of slow anion channels in the plasma membrane of guard cells (large nitrate permeability). Plant Physiol. **106:** 383–391.

Schneider, C.A., Rasband, W.S., and Eliceiri, K.W. (2012). NIH Image to ImageJ: 25 years of image analysis. Nat. Methods **9:** 671–675.

Shelden, M.C., Howitt, S.M., Kaiser, B.N., and Tyerman, S.D. (2009). Identification and functional characterisation of aquaporins in the grapevine, *Vitis vinifera*. Funct. Plant Biol. **36:** 1065–1078.

Somersalo, E., Occhipinti, R., Boron, W.F., and Calvetti, D. (2012). A reaction-diffusion model of CO_2 influx into an oocyte. J. Theor. Biol. **309:** 185–203.

Speight, J.G. (2005). Lange's Handbook of Chemistry, (New York: McGraw-Hill Press).

Tian, W., et al. (2015). A molecular pathway for CO_2 response in Arabidopsis guard cells. Nat. Commun. **6:** 6057.

Uehlein, N., Lovisolo, C., Siefritz, F., and Kaldenhoff, R. (2003). The tobacco aquaporin NtAQP1 is a membrane CO_2 pore with physiological functions. Nature **425:** 734–737.

Uehlein, N., Otto, B., Hanson, D.T., Fischer, M., McDowell, N., and Kaldenhoff, R. (2008). Function of *Nicotiana tabacum* aquaporins as chloroplast gas pores challenges the concept of membrane CO_2 permeability. Plant Cell **20:** 648–657.

Uehlein, N., Sperling, H., Heckwolf, M., and Kaldenhoff, R. (2012). The Arabidopsis aquaporin PIP1;2 rules cellular CO_2 uptake. Plant Cell Environ. **35:** 1077–1083.

Vahisalu, T., Kollist, H., Wang, Y.F., Nishimura, N., Chan, W.Y., Valerio, G., Lamminmäki, A., Brosché, M., Moldau, H., Desikan, R., Schroeder, J.I., and Kangasjärvi, J. (2008). SLAC1 is required for plant guard cell S-type anion channel function in stomatal signalling. Nature **452:** 487–491.

Waadt, R., Hitomi, K., Nishimura, N., Hitomi, C., Adams, S.R., Getzoff, E.D., and Schroeder, J.I. (2014). FRET-based reporters for the direct visualization of abscisic acid concentration changes and distribution in *Arabidopsis.* eLife **3:** e01739.

Walter, M., Chaban, C., Schütze, K., Batistic, O., Weckermann, K., Näke, C., Blazevic, D., Grefen, C., Schumacher, K., Oecking, C., Harter, K., and Kudla, J. (2004). Visualization of protein interactions in living plant cells using bimolecular fluorescence complementation. Plant J. **40:** 428–438.

Wang, Y., Cohen, J., Boron, W.F., Schulten, K., and Tajkhorshid, E. (2007). Exploring gas permeability of cellular membranes and membrane channels with molecular dynamics. J. Struct. Biol. **157:** 534–544.

Webb, A.A., and Hetherington, A.M. (1997). Convergence of the abscisic acid, CO_2, and extracellular calcium signal transduction pathways in stomatal guard cells. Plant Physiol. **114:** 1557–1560.

Xue, S., Hu, H., Ries, A., Merilo, E., Kollist, H., and Schroeder, J.I. (2011). Central functions of bicarbonate in S-type anion channel activation and OST1 protein kinase in CO_2 signal transduction in guard cell. EMBO J. **30:** 1645–1658.

Yamamoto, Y., Negi, J., Wang, C., Isogai, Y., Schroeder, J.I., and Iba, K. (2016). The transmembrane region of guard cell SLAC1 channels perceives CO_2 signals via an ABA-independent pathway in *Arabidopsis.* Plant Cell 28: 10.1105/tpc.15.00583.

Yang, Y., Costa, A., Leonhardt, N., Siegel, R.S., and Schroeder, J.I. (2008). Isolation of a strong Arabidopsis guard cell promoter and its potential as a research tool. Plant Methods **4:** 6.

Zhao, Z., Zhang, W., Stanley, B.A., and Assmann, S.M. (2008). Functional proteomics of *Arabidopsis thaliana* guard cells uncovers new stomatal signaling pathways. Plant Cell **20:** 3210–3226.